EFFECT OF POWDER FLOW PROPERTIES ON THE PROCESS PERFORMANCE OF LOSS-IN-WEIGHT FEEDERS

By

PENGBO LI

A thesis submitted to the

Graduate School – New Brunswick

Rutgers, The State University of New Jersey

In partial fulfillment of the requirement

For the degree of

Master of Science

Graduate Program in Chemical and Biochemical Engineering

Written under the direction of

Dr. Fernando J. Muzzio

And approved by

_____

_____

_____

_____

New Brunswick, New Jersey

May, 2015

ABSTRACT OF THE THESIS

Effect of powder flow properties on the process performance of loss-in-weight feeders

By PENGBO LI

Thesis Director:

Dr. Fernando J. Muzzio

This thesis focuses on the flow properties of catalyst support materials and their behaviors in loss-in-weight feeders. The flow properties of nine common catalyst support materials were measured: Coarse Alumina, Fine Alumina, Fine Zeolite, Molybdenum oxide, Satintone, Titania, Versal 300, Y-655 and Zeolite. The flow properties included particle size distribution, wet and dry impedance at 100Hz, FT4 tests including shear cell (cohesion, Unconfined Yield Strength UYS, Major Principle Stress MPS and Flow Function FF), compressibility (Conditioned Bulk Density CBD and percentage change in volume after compression CPS), permeability (Pressure Drop PD), Stability and Variable Flow Rate (Rep+VFR) (Basic Flowability Energy BFE, Stability Index SI, Flow Rate Index FRI and Special Energy SE). Principal component analysis was performed to analyze these flow properties and find the most

representative materials for feeder tests (Coarse Alumina, Fine Alumina and Satintone). Different material properties were found to be correlated using multivariate analysis. The feeding performance of the Coarse Alumina, Fine Alumina and Satintone was measured using Schenck Accurate Purefeed AP-300 loss-in-weight feeder. The instantaneous feedrate was obtained every 0.1s. The relative standard deviation (RSD) was calculated and used to characterize the feeder behaviors. This makes a better understanding of the impact of powder material properties, device design, and operating conditions on the variability in powder feed rate in loss-in-weight feeders. The flow properties of catalyst support materials were characterized systematically and their effects on the process performance in loss-in-weight feeders could be used to aid in the proper selection of feeder tooling for a given powder.

Acknowledgement

I would like to thank the guidance and resources provided by my advisor Dr. Fernando J. Muzzio. He is always responsible and supportive and teaches me a lot not only on research but also others that will help me a lot in my future. And I also would like to thank Dr. Sara Koynov, Yifan Wang, Dr. Bill Engisch, Sarang Oka and Dr. SavithaPanikar for their help with experimental methods and difficulties I faced in my research. Furthermore, I would like to acknowledge the Muzzio group for the wonderful experience I had during my master career.

I want to thank my parents for their trust and support for my study abroad. I want to thank my friends I met in Rutgers that you rich my life in Rutgers.

Table of Contents

1 Introduction

The catalyst support material is a solid with a high surface area, attached by a catalyst. The reactivity of heterogeneous catalysts and nanomaterial-based catalysts occurs at the surface atoms. Hence, it creates a great effort with the maximum surface area of a catalyst. The catalyst support materials have been widely used in various fields for enhancing the mechanical support of catalyst, increasing the effective catalyst surface, improving the thermal stability, reducing the amount of catalyst and lowing the costs. Although having been widely used in industry, there is still a problem in powder-based continuous manufacturing process for its requirement of high degree accuracy in product composition. Producers often focus on suboptimal batch manufacturing due to lack of understanding powder flow behavior in continuous manufacturing [1]. This makes a better understanding of the flow properties of catalyst support materials necessary to deal with the handling of bulk solids for industrial processes. Schneider et al. [2] used a model die-shoe filling system to evaluate the flowability of seven pharmaceutical powders and identified the dominant mechanism for a given powder, environment, geometry and shoe kinematics. Abdullah et al. [3] found a new non-aerated method, where Cohesion Index (CI) was measured, reliable in predicting flow characteristics. Jiang et al. [4] developed an automatic measurement system based on vibrating capillary method which has a high resolution to evaluate the flow properties of powder. Emery et al. [5] found that increasing moisture content non-linearly decreased the flowability of Hydroxypropyl Methylcellulose and non-linearly increased the flowability of Aspartame. The Jenike shear test is the only acceptable test of flowability for complex flow behavior. Faqih et al. [6] found that gravitational displacement Rheometer (GDR) is an effective and convenient tool for examining flow properties of pharmaceutical materials.

There are many studies focusing on characterizing flow properties of powders such as particle size distribution, density, impedance, cohesion. Nonetheless, there are still other effects on powders' flow behaviors during a manufacturing process, such as

loading experience (gravity, vibration, body forces), operating conditions (temperature, moisture or dry), current state of the powder (tapped, consolidated, aerated) [2]. There is not a unified way to characterize flow properties for all operations. Dawes et al. [7] found that the addition of magnesium stearate as a lubricant can increase ribbon mass throughput with two "knurled" rollers but decrease if one of them is smooth. Vanarase et al. [8] found bulk density to be the key material property that affects mean residence time during mixing. On the other hand, cohesion has greater effects on axial dispersion coefficient. Zhou et al. [9] found that the improvement in powder flowability was dependent on the coating parameters, namely processing speed and processing time duration by dry coating various commercial fine lactose powders. Sinka et al. [10] changed the tablet processing parameters to find the effects on tablets properties and figured out the optimal conditions with powder flow properties. There are lots of persons studying powders' behaviors in different kinds of operations, like coating, tableting, mixing. But few focused on powders' flow behaviors in feeders, especially catalyst support materials in feeders. Feeder as a fundamental equipment, is almost necessary for all the operations in industrial manufacture. Raw materials or semi-finished products are fed to the downstream production. While for large scales of operation, inaccuracies in ingredient are not a big problem, at the small flowrates (0.5-100kg/h) they may cause large variability for subsequent unit operation, which should be avoided.

Loss-in-weight feeders are feeders that can better control feedrate and minimize flow variability caused by bulk density changes associated with the empty of the feeding hopper. This work aims to predict the performances of catalyst support materials in loss-in-weight feeder. In order to find out the relationship between the material flow properties and the feeding tools, a dataset library was established, including nine materials and their flow properties to help systematic understanding and predicting manufacturing process performance. For something new, it can be compared with the existing ones in the library. This will make it easy to characterize and predict the new material's flow behavior in feeders. Meanwhile, it is helpful for other unit operation.

In this work, we applied several tests to measure the materials' flow properties, particle size distribution, dry and wet impedance, FT4 test such as shear cell, Stability and Variable Flow Rate (Rep+VFR), compressibility, permeability, trying to find the interior relations between these flow properties. Statistical analysis method principal component analysis (PCA) was used to cluster the materials and three different materials were selected. Their behaviors in feeders were characterized and the relationship between the feeder tools and flow properties was determined.

2 Methods

2.1 Flow property measurement

A thorough understanding of a bulk material's flow properties and its flowability are crucial for identifying the cause of poor flow, powder flooding or rate limitations, segregation, or product non-uniformity. Key bulk material flow properties were measured for troubleshooting problems.

2.1.1 FT4 Powder Rheometer

The FT4 Powder Rheometer as shown in Fig 2-1 designed by FreemanTechnology was used to measure the materials' flow properties including compressibility, permeability, shear cell and Rep+VFR tests. It simulates the process conditions to quantify the powder's response to each variable. Krantz et al. [11] compared the static and dynamic testing methods for characterizing powder flow and used FT4 as the static method to better predict agglomeration with cohesion. FT4 was also used to measure particle shape and size [12], study discrete element simulation (DEM) [13], and measure the flow properties of consolidated, conditioned and aerated powders [14]. The sample is placed in a Split Vessels as shown in Fig 2-2, which allows a precise volume to be attained and the density of sample can be measured with unprecedented levels of accuracy. A precision 'blade', or impeller as shown in Fig 2-3, is needed for the tests. Before each test cycle, a preparation step called conditioning process performs to prepare the sample for the following measurement and remove any effects remained in the sample by rotating and moving the impeller downwards and upwards through the powder three times.

Fig 2-1 FT4 Powder Rheometer

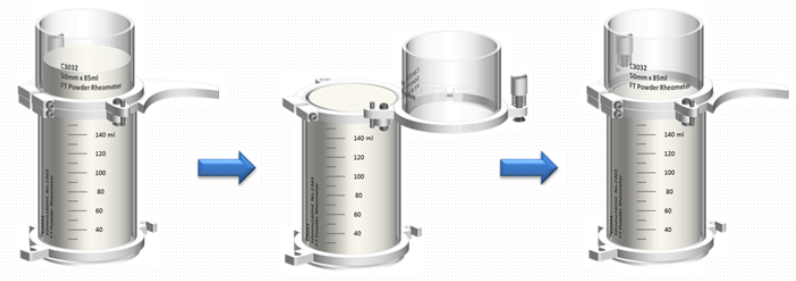

Figure 2-2 Split Vessel for FT4 test

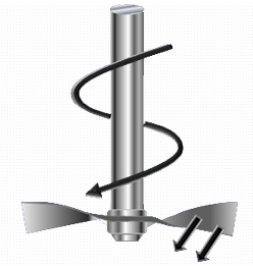

Figure 2-3 impeller for FT4 test

(1) Compressibility is a measure of how density changes as a function of applied normal stress. A vented piston is used to apply a normal force from 0.5 to 15 kPa onto the sample. Conditioned Bulk Density (CBD) and Percentage change in volume after compression (CPS) were obtained.

CBD is the powder sample's density with free of localized stress and any excess air.

(2) Permeability is a measure of how easily material can transmit a fluid (in this case air) through its bulk. The process is similar to the compressibility except that air with constant velocity goes through the sample during the compression. Pressure

Drop (PD) was obtained.

PD represents the pressure drop across the powder bed versus normal stress, for a constant air velocity.

(3) Shear properties are important for understanding how easily a previously at rest, consolidated powder will begin to flow. Measuring the shear properties will provide important information as to whether the powder will flow through the process or whether bridging, blockages and stoppages are likely. After conditioning, the sample will be compressed with the vented piston to a selected condition, called initial consolidation stress. The shear head in Fig 2-4 moves downwards inserting the blades into the powder and induces a normal stress as the shear head face contacts the top of the powder. After the required normal stress σ is established, the shear head begins rotation slowly to induce a shear stress τ. It will increase the shear stress until the bed fails or shears, at which time a maximum shear stress is observed. The maximum shear stress is the yield point. The sample will be pre-sheared at the maximum normal stress until the shear stress reaches steady state. Then the sample will be sheared to obtain five yield points with different normal stress and shear stress. Cohesion, Unconfined Yield Strength (UYS), Major Principle Stress (MPS), Flow Function (FF) at 3 kPa, 6 kPa, 9 kPa and 15 kPa initial consolidation stress were obtained.

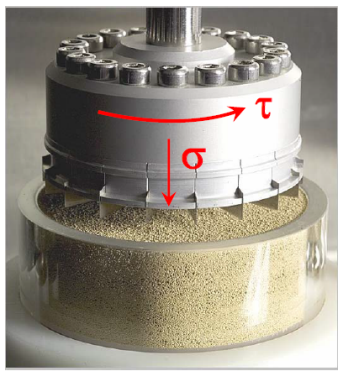

Figure 2-4 shear head for shear cell test

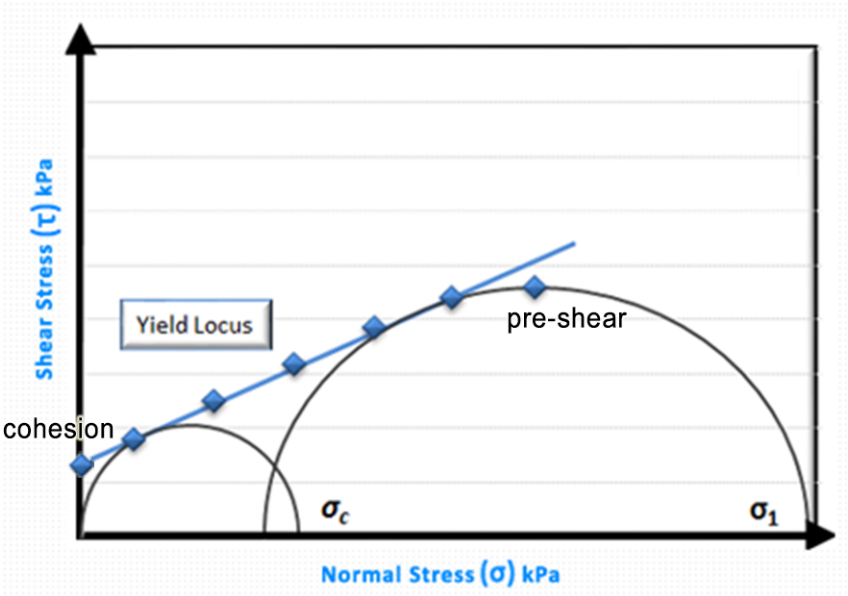

Figure 2-5 sample of analyzing shear cell data

In Fig 2-5, the five yield points build the yield locus. It can be seen as linear. Two semi-circles are tangent of the yield locus.

Cohesion: the point of intersection of the yield locus with the normal stress zero.

UYS (Sigma c)

MPS (Sigma 1)

FF, the ratio of MPS to UYS

(4) Stability (Rep) and Variable Flow Rate (VFR) is used to describe the stability of a powder in a system and the sensitivity of a powder to flow rate. It's a combination of conditioning and test cycles. In the test cycle, the impeller will rotate and move downwards and upwards through the sample with a constant tipspeed to measure the energy required. The condition and test cycle will process 7 times with the testing blade tipspeed 100 mm/s to describe the stability and 4 times with the testing blade tipspeed decreased from 100 to 10 mm/s to describe the sensitivity of the sample to flow rate. Basic Flowability Energy (BFE), Stability Index (SI), Flow Rate Index (FRI) and Specific Energy (SE) were obtained.

BFE is the energy required to establish a particular flow pattern in a conditioned, precise volume of powder. It's calculated from the work done in moving the blade

through the powder from the top of the vessel to the bottom during the downward traverse.

SI is used the measure the stability of a powder. If the powder changes for any reason, a trend reflecting this change is usually observed.

FRI is used to characterize the sensitivity of a powder to flow rate change.

SE is a dynamic measurement, similar to the BFE. The major difference is that the energy is derived when the blade is moving upwards, from the bottom of the powder to the top.

BFE=Energy Test 7

Stability Index (SI)= Energy Test 7/Energy Test 1

Flow Rate Index (FRI)=Energy Test 11/Energy Test 8

Specific Energy (SE) =(Up Energy Cycle 6+Up Energy Cycle 7)/2/Split Mass

2.1.2 Impedance of powder

Impedance as an electrical property of powder, represents electric conductivity. That is related to the frequent particle-particle contacts and finally reflects on the cohesive effects [15]. Abiad et al. [16] and Pingali et al. [17] also used impedance as an important parameter to characterize powders' flow behavior in their study. In this work, the impedance of powder was measured by a TREK Model 610E (Fig 2-6) from TREK as the high-voltage supply and a DSO3062A (Fig 2-7) from KEYSIGHT Technologies as an oscilloscope. As shown in Fig 2-8, the sample (40g) was loaded in a Faraday cup. The electrical signal was passed through the powder by applying a sinusoidal voltage to the top and bottom electrodes of the cup. The output signal was recorded using the oscilloscope. Peak to peak voltage and current readings were recorded using oscilloscope. The impedance was measured as the modular ratio of the amplitudes of the applied voltage and the resulting current.

Fig 2-6 TREK Model 610 E

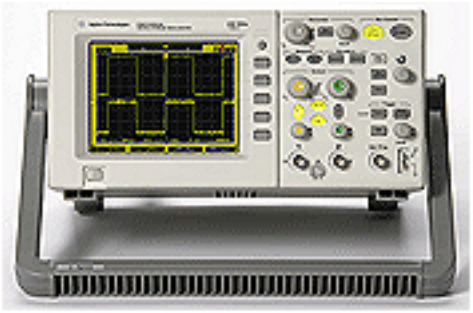

Fig 2-7 DSO3062A

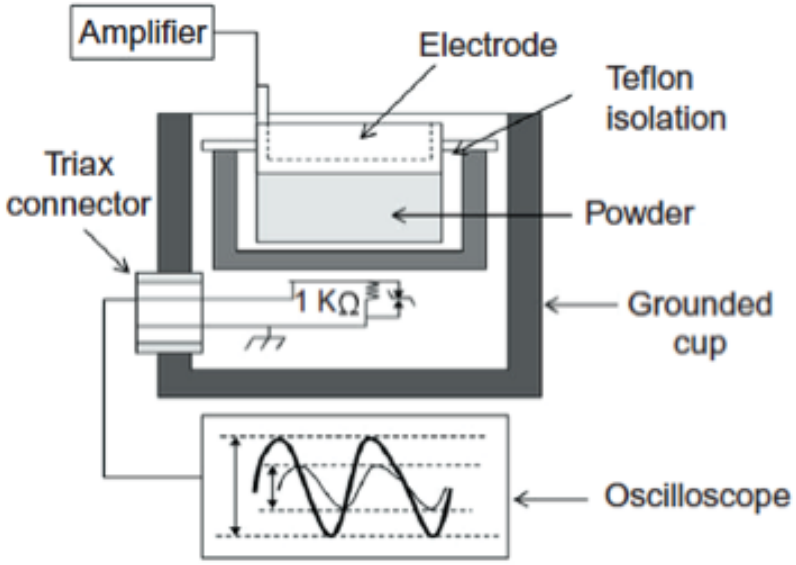

Figure 2-8 impedance measurement with oscilloscope, Faraday cup and amplifier

2.1.3 Particle size distribution

The particle size distribution can affect basic unit operations such as mixing, filtration, flowing through hoppers [18]. It has significant effects on powder flow properties. Sarragca et al. [19] compared three ways, NIR spectra, flowability properties and the concentrations of the components present in the samples, to predict particle size distribution and found NIR method the best. Sarrate et al. [20] used spray drying technology to alter the particle size distribution. Wiens and Pugsley [21] studied hydrodynamics in a conical fluidized bed with two kinds of particle size. In

this work, particle size distribution was measured with a Beckman-Coulter LS 13 320 series laser diffraction particle size analyzer (Fig 2-9). The Tornado Dry Powder dispersing system was used to introduce the sample into the machine. The agglomerates will be broken during tests. Fraunhofer's model was used for light scattering data analysis.

Fig 2-9 Beckman-Coulter LS 13 320

2.2 Principal component analysis

Nine common catalyst support materials are involved in the study. They may have some similar flow properties with each other and can be characterized in the same way in feeders and other unit operations. To save time and money, we planned to identify a subset of 3-4 materials according to statistical analysis methods based on the measurement of material flow properties.

Principal component analysis (PCA) is a multivariate statistical analysis method that electssome important variables by a linear transformation of more variables. In real problems, in order to analyze the problem, there will always be a lot of variables associated to reflect some information of the problem. Too many variables will increase the complexity of the problem. It's better to find a relationship between the variables and minimize them into a set of several new independent variables. Lin et al. [22] used PCA to identify the reference spectra of a pharmaceutical tablet's constituent compounds from Raman spectroscopic data. Adamska et al. [23] applied PCA to select the solubility parameters for characterizing pharmaceutical excipients.

Qu et al. [24] applied PCA to reduce input variables of the adaptive neuron-fuzzy inference system (ANFIS). PCA are widely used for its practicability. PCA was used to help better understand the correlations between flow behaviors and select representative materials for further study.

2.3 Loss-in-weight feeder

A loss-in-weight feeder Schenck Accurate Purefeed AP-300 was used. It consists of three parts: volumetric feeder, weighing platform (load cell), and gravimetric controller. As shown in Fig 2-10, the weighing platform under the volumetric feeder is used to measure the mass of the feeder and the hopper on top. While the powder is feeding, the load cell will send a signal of instantaneous weight to the controller. Comparing the signal with the original setpoint, the controller will adjust the rotating speed of screw that dispenses powder in the feeder to maintain the feedrate constant.

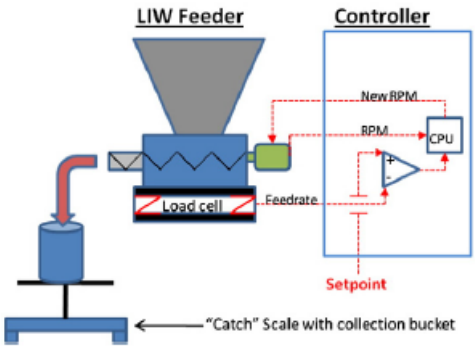

Figure 2-10 diagram of the main components of loss-in-weight feeder

Figure 2-11 loss-in-weight feeder AP-300

A Schenck Accurate AccPro II was used as a "catch" scale for characterization of the loss-in-weight feeders' performance. It is necessary because the internal load cell measurement uses different filtering algorithms to pre-treat the gravimetric signal, which may be different between different feeders [1]. AccPro II is a PC Excel program that obtains weight readings from a 10kg strain gage load cell through the

Schenck DISOBOX summing box. It will read the weight every 0.1s, which is enough to catch small variations associated with feeding powders.

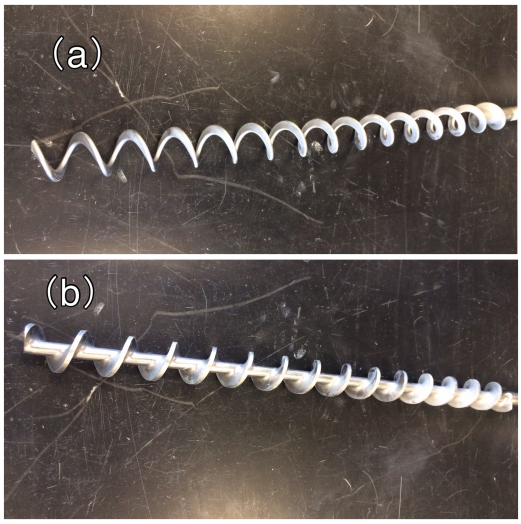

Figure 2-11 screw designs. (a) open helical screw called helix. (b) helical screw with center shaft called screw.

Figure 2-12 cross screen

The selected materials were fed by different combination of feeder tools. Two kinds of screw are shown in Fig 2-11 and one screen is shown in Fig 2-12. It gives 4 combination for each material, helix without screen, helix with screen, screw without screen, screw with screen. For each material with each combination, a calibration was performed first to determine the capacity of the feeder. Then the setpoints of feedrate covered about 80% of the capacity with an interval 5 kg/h. Each test ran ten minutes to make the data convincing. This is long enough for feeder reaching steady state and lasting a long time.

The surroundings may affect the feeders' stability, like breeze. Increasing the time interval will eliminate the effect of surroundings. However, the residence time of the subsequent unit operations should be considered. The sampling interval should be short enough to detect fluctuations that are pertinent to the process. The sampling interval needs to be shorter than the residence time of the subsequent unit operations. Therefore, 0.1s and 1s intervals were applied in this work.

The mass feedrate is calculated by

$$\dot{m} = \frac{\Delta m_i}{\Delta t}$$

Where $\dot{m}$ is the mass feedrate, Δm_i is the weight different every interval and Δt is the interval.

From all the mass feedrate at each interval, a distribution can be determined. From this distribution, the standard deviation σ and relative standard deviation RSD can be calculated to characterize the catalytic behavior.

$$\sigma = \sqrt{\frac{\sum_{i=1}^{n}(\dot{m}_i - \overline{\dot{m}})}{n-1}}$$

$$\text{RSD} = \frac{\sigma}{\overline{\dot{m}}}$$

Where $\overline{\dot{m}}$ is the arithmetic mean mass feedrate of the distribution and n is the number of samples in the distribution.

3 Results and discussion

3.1 Principal component analysis

Table 3-1 is the flow properties measured of nine common catalyst support materials. The cohesion of Versal 300 at 3,6,9 kPa are negative, which make the followed UYS and FF zero. This suggests that Versal 300 is close to free flowing. The Dry impedance of Zeolite, Wet impedance of Molybdenum oxide, Titania and Zeolite are missing because the current of the test are too large that over the limit and can not be shown by the oscilloscope. It's a large work and too many variables are involved.

Table 3-1 flow properties measured of nine materials

	Coarse Alumina	Fine Alumina	Fine Zeolite	Molybdenum oxide	Satintone	Titania	Versal 300	Y-655	Zeolite
CPS, % 15.0kPa	3.91	29.59	14.68	25.01	36.39	36.55	4.18	25.90	35.02
CBD, g/ml	0.96	0.31	0.85	1.39	0.52	0.35	0.34	0.31	0.25
PD,mBar-15.0kPa	1.46	32.88	8.63	7.95	4.14	3.43	1.43	10.01	4.85
Cohesion,kPa -3kPa	0.12	0.42	0.51	1.02	0.93	0.54	-0.04	0.82	0.81
UYS, kPa-3kPa	0.42	1.47	1.60	4.27	3.74	2.58	0	2.90	2.97
MPS, kPa-3kPa	4.70	5.47	4.42	7.23	7.18	7.34	4.260	6.01	6.20
FF-3kPa	11.29	3.72	2.77	1.69	1.92	2.85	0	2.07	2.09
Cohesion,kPa -6kPa	0.07	0.78	0.50	1.48	1.23	0.30	-0.09	1.18	1.78
UYS, kPa-6kPa	0.26	2.62	1.59	6.30	4.96	1.52	0	4.17	6.32
MPS, kPa-6kPa	9.23	10.52	8.63	13.57	13.44	13.63	8.33	11.19	12.50
FF-6kPa	35.85	4.01	5.42	2.16	2.73	9.58	0	2.68	1.99
Cohesion,kPa -9kPa	0.16	0.98	0.56	2.23	1.32	0.66	-0.18	1.51	1.84
UYS, kPa-9kPa	0.54	3.31	1.73	8.93	5.34	3.04	0	5.27	6.53
MPS,	13.42	15.63	12.89	20.32	19.97	19.71	13.10	16.47	18.47

kPa-9kPa									
FF-9kPa	24.86	4.73	7.47	2.28	3.74	6.52	0	3.14	2.84
Cohesion,kPa -15kPa	0.37	1.39	0.49	2.45	1.01	-0.004	0.28	1.84	1.72
UYS, kPa-15kPa	1.20	4.57	1.53	10.50	4.40	0.36	0.85	6.51	6.39
MPS, kPa-15kPa	22.78	25.26	21.16	32.08	31.20	30.42	22.21	26.17	28.72
FF-15kPa	19.11	5.53	14.16	3.06	7.25	61.19	26.49	4.06	4.50
BFE, mJ	2070.18	212.39	573.96	4218.50	858.75	541.58	602.17	234.49	401.41
SI	0.98	1.20	1.42	1.09	1.09	1.01	0.97	1.14	0.99
FRI	1.02	1.92	1.74	1.29	1.53	1.68	0.95	2.03	1.68
SE, mJ/g	5.85	6.94	7.44	12.17	14.88	10.96	4.50	8.09	9.92
Dried Impedance at 100Hz	24.04	46.30	19.23	27.78	50	31.25	43.10	36.07	
Wet Impedance at 100Hz	2.84	36.76	6.75		62.5		7.65	38.25	
d10	11.16	0.99	0.94	0.76	0.92	0.69	12.35	0.80	0.77
d50	59.37	4.07	3.86	3.71	6.10	2.99	147.83	2.33	2.99
d90	122.19	11.46	5.82	10.31	21.14	10.13	560.05	7.59	10.43

3.1.1 PCA of 9 materials

Table 3-1 shows the materials' flow properties including particle size distribution, dry and wet impedance, and other data measured from FT4 test such as shear cell, Rep+VFR, compressibility, permeability. Non-linear Iterative Partial Least Squares algorithm (NIPALS) PCA was performed. The data were mean centered so that the first principal component describes the direction of maximum variance. The measurements were normalized to make the data similar in scale. The first principal component explains 52% of the variability in the data and the second principal component explains 14%. The first and second principal components explain 66% of the variability and the third principal component explains 10%. But the first and second principal components were enough to classify these materials for feeder tests. There is no need to find the precise position of each material in the model.

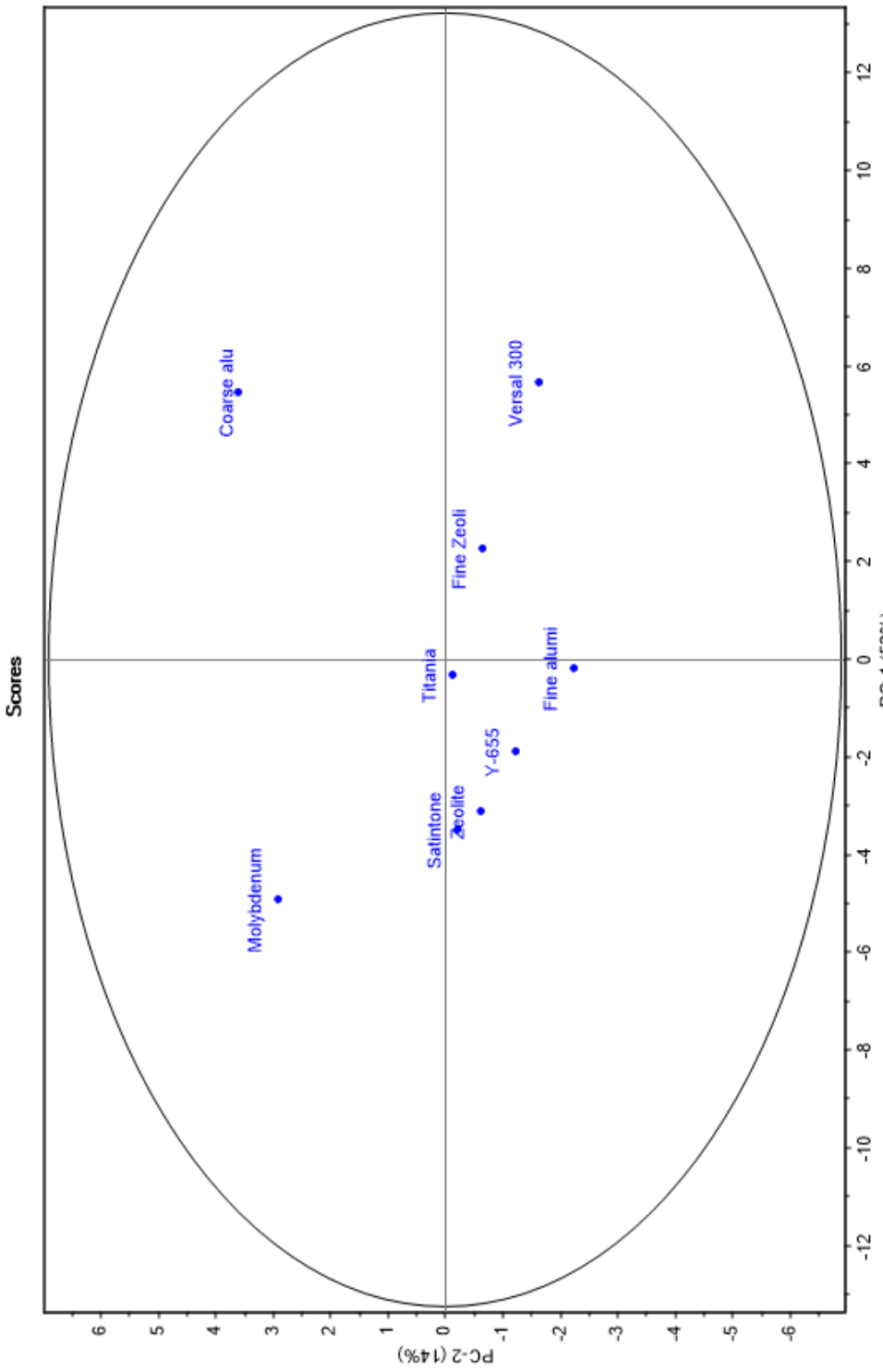

Figure 3-1 Scores plot of PCA of 9 materials

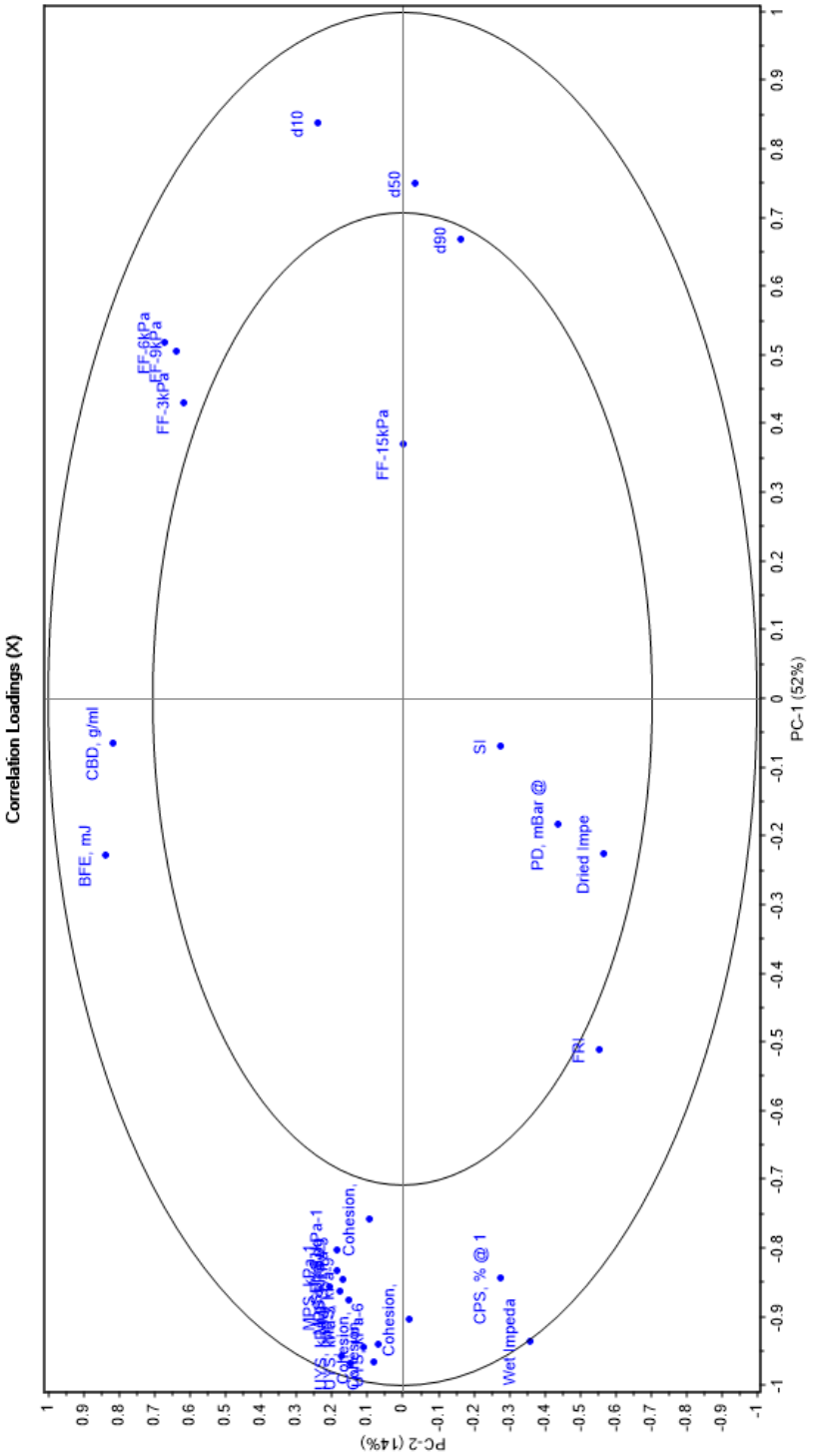

Figure 3-2 Correlation loadings of PCA of 9 materials

From Fig 3-2, we can see that SI, PD, Dried Impedance and FF-15 kPa lie in the inner circle, suggesting that they have small contribution to discriminating for the samples in this model. Most measurements in the outer circle are also correlated to each other. For example, BFE and CBD are at the top of the ellipse. They have positively correlation to each other. Cohesions are at the left. D50 is at the right. They have negative correlation to each other. BFE and Cohesion are independent to each other.

From Fig 3-1 we can see a triangular structure with three apexes corresponding to Molybdenum oxide, Coarse Alumina and Fine Alumina. Since Molybdenum oxide is no longer commercially available in industry, Satintone was selected instead. Coarse Alumina and Versal 300 are similar based on PC-1 and different based on PC-2. Since cohesion, UYS, MPS and FF have large contribution to PC-1 and the cohesion of Versal 300 at 3,6,9 kPa are negative, PCA of 8 materials should be performed.

3.1.2 PCA of 8 materials

PCA was performed again without Versal 300. In this model, the first principal component explained 52% of the variability and the second explained 18%.

From Fig 3-3, Coarse Alumina, Fine Alumina and Satintone were selected for feeder tests.

From Fig 3-4, the outer ellipse is the unit-circle and indicates 100% explained variance. The inner ellipse indicates 50% of explained variance. It can be seen that measurements are highly correlated.

Since measurements were highly correlated, model can be reduced to fewer variables. The following measurements were used in the reduced model: CPS% from compressibility test, cohesion and flow function coefficient at 9 kpa, basic flow energy (BFE) and flow rate index (FRI), and wet impedance at 100Hz.

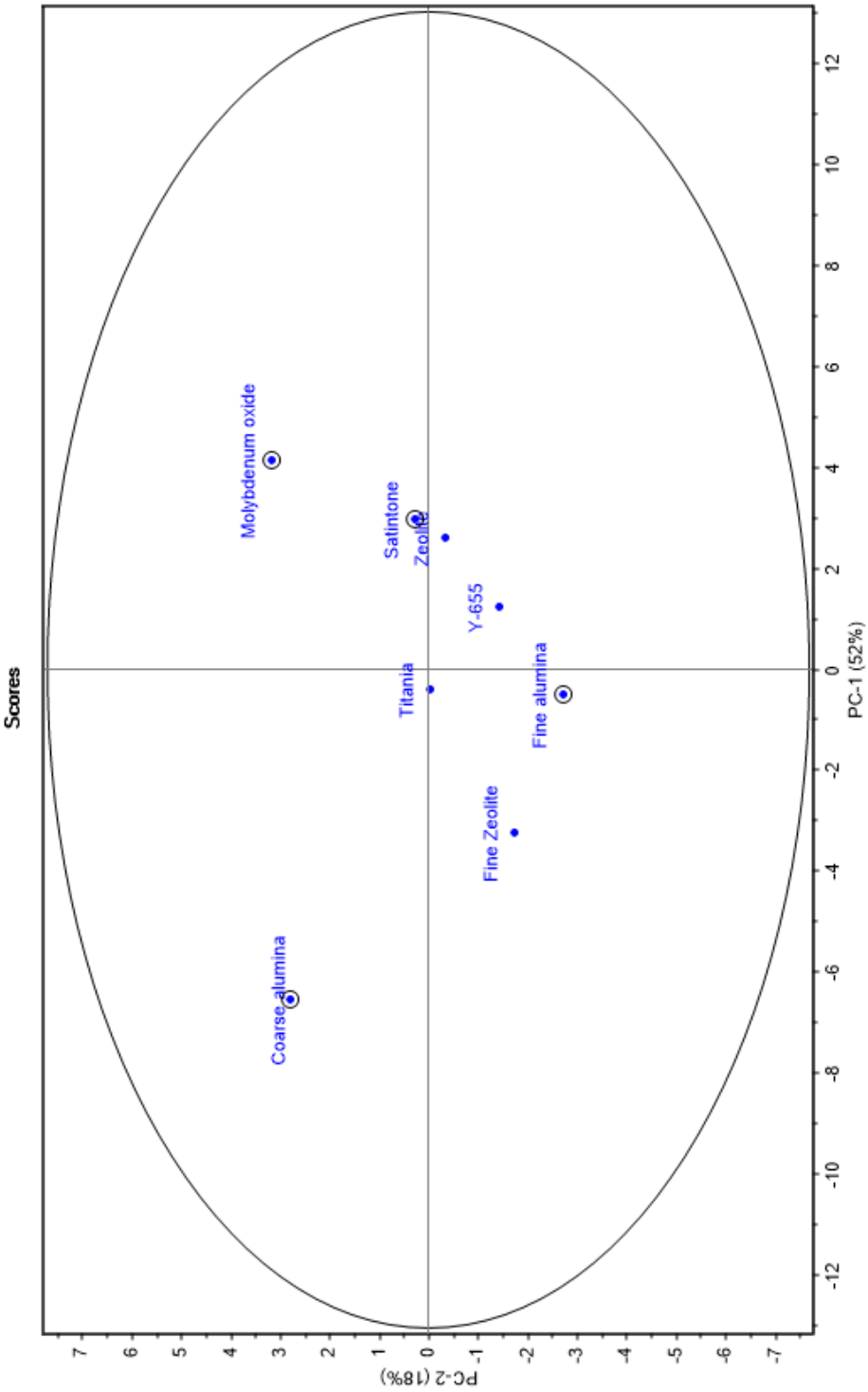

Figure 3-3 scores plot of PCA of 8 materials

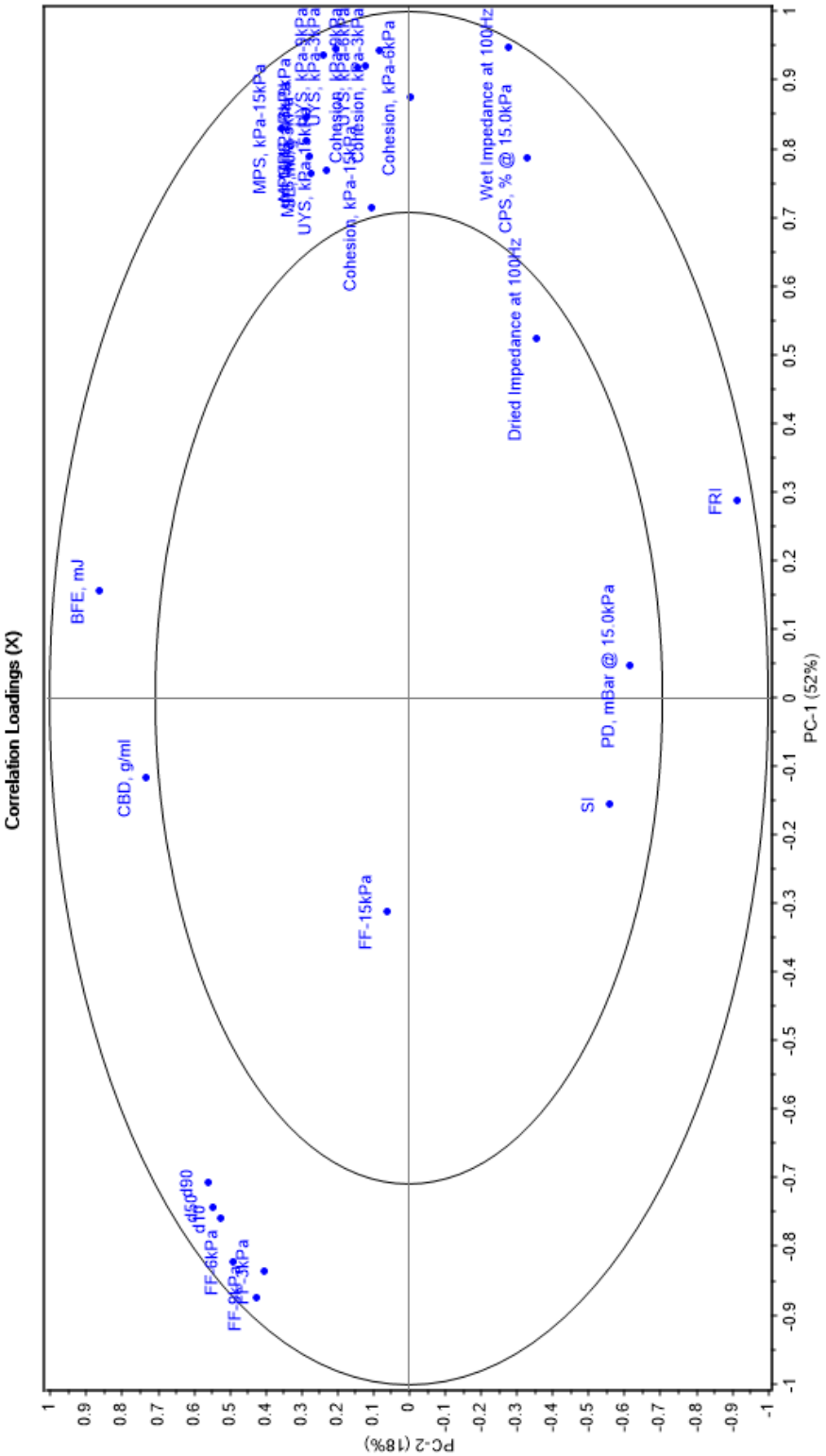

Figure 3-4 correlation loadings of PCA of 8 materials

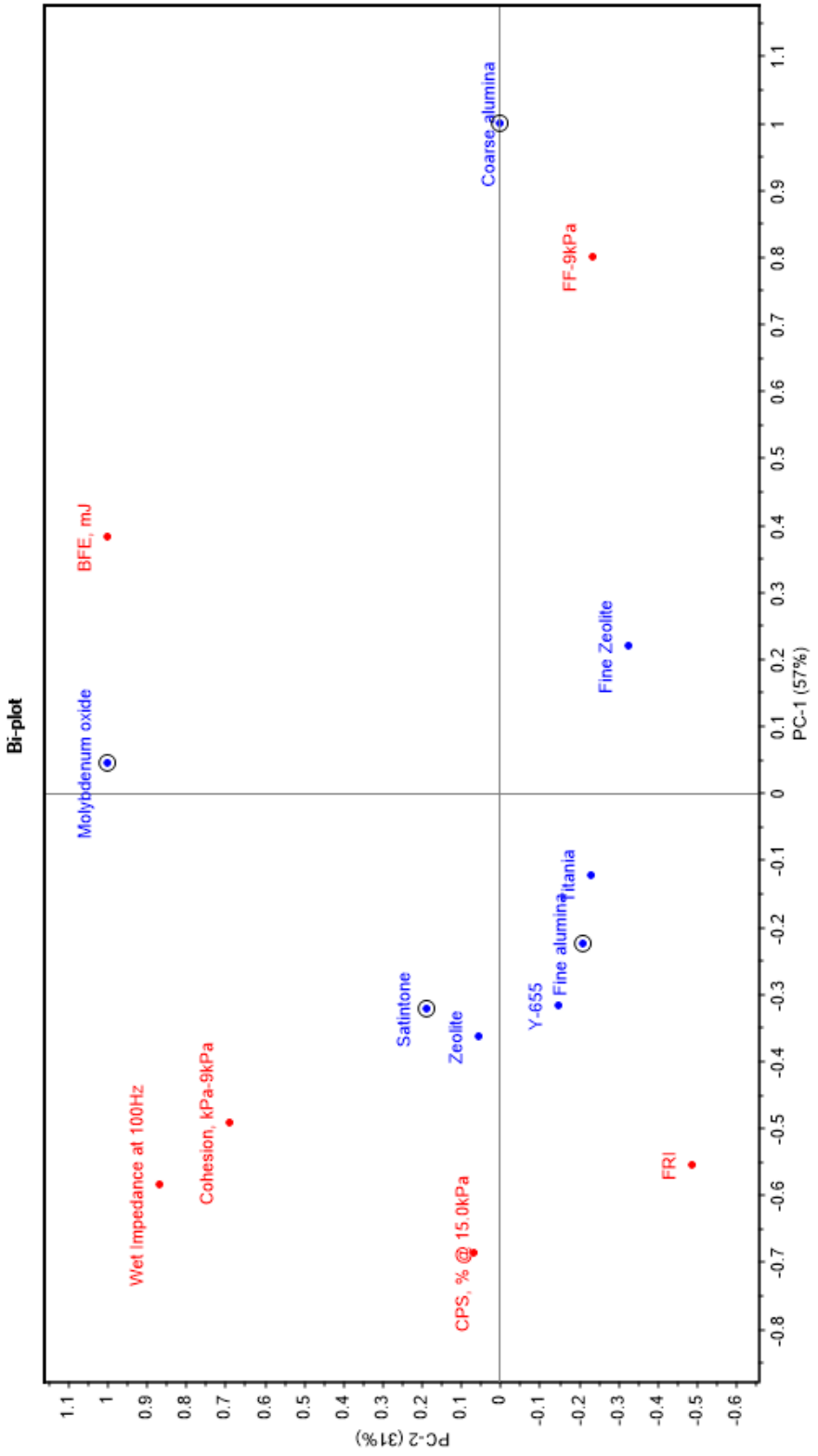

Figure 3-5 Bi-plot of reduced model of PCA

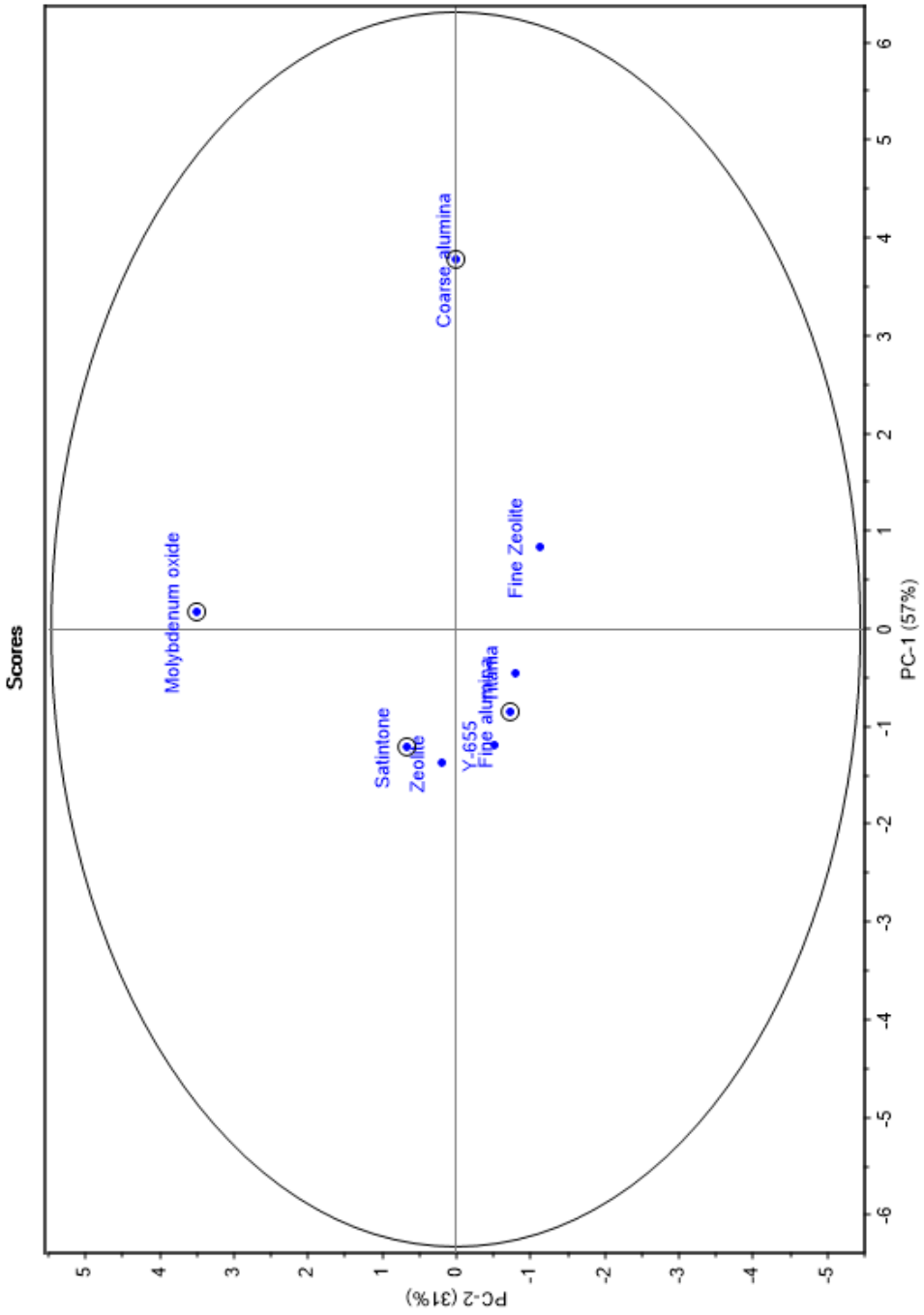

Figure 3-6 scores plot of reduced model of PCA

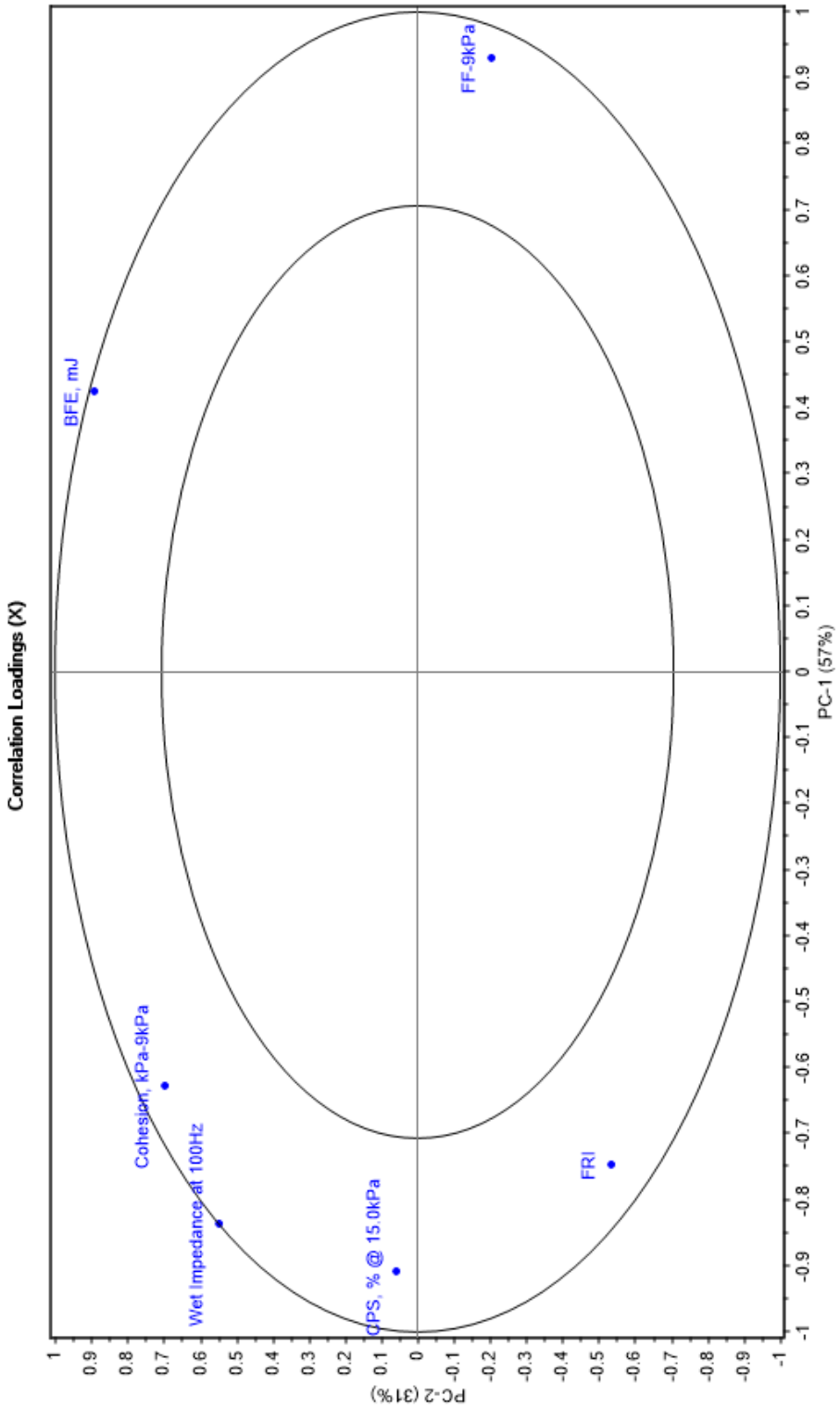

Figure 3-7 correlation loadings of reduced model of PCA

3.1.3 CBD, BFE and FRI

From Fig 3-4 we can see that CBD and BFE have a positive correlation to each other. They are on the top of the correlation loadings ellipse. CBD is conditioned bulk density that is measured by FT4 creating a low stress, homogeneous packing state. It reflects the normal condition of a powder without localized stress and excess air. A Large CBD means large density of the powder or low air content or both. A Small CBD means small density of the powder or high air content or both. BFE, the Basic Flowability Energy, is the energy required for a blade rotating and moving downwards and upwards through the powder, which also generates a compressive, relatively high stress flow mode in the powder. It's easy to think that for large CBD, the resistance will be large for a blade to move inside the powder. The blade needs to push powder on its way to the sides. Low air content or large powder density will increase the difficulty level of the movement, resulting in a large BFE value. On the other hand, FRI, Flow Rate Index, on the bottom of the ellipse, reflects the sensitivity of a powder to flow rate. Cohesive powders are usually more sensitive to flow rate because they have high air content. And high air content, in a way, means small CBD. That's why CBD and BFE have negative correlation with FRI. It's nonlinear because the density of the powder has influence and it's also shown in Fig 3-4 that FRI and CBD have a little difference in PC-1.

Table 3-2 data of CBD, BFE and FRI

	coarse alumina	fine alumina	Fine Zeolite	Molybdenum oxide	Satintone	titania	Versal 300	Y-655	Zeolite
CBD g/ml	0.96	0.31	0.86	1.39	0.52	0.35	0.34	0.31	0.25
BFE mJ	2070.18	212.39	573.96	4218.50	858.75	541.58	602.17	234.49	401.41
FRI	1.02	1.92	1.74	1.29	1.53	1.68	0.95	2.03	1.68

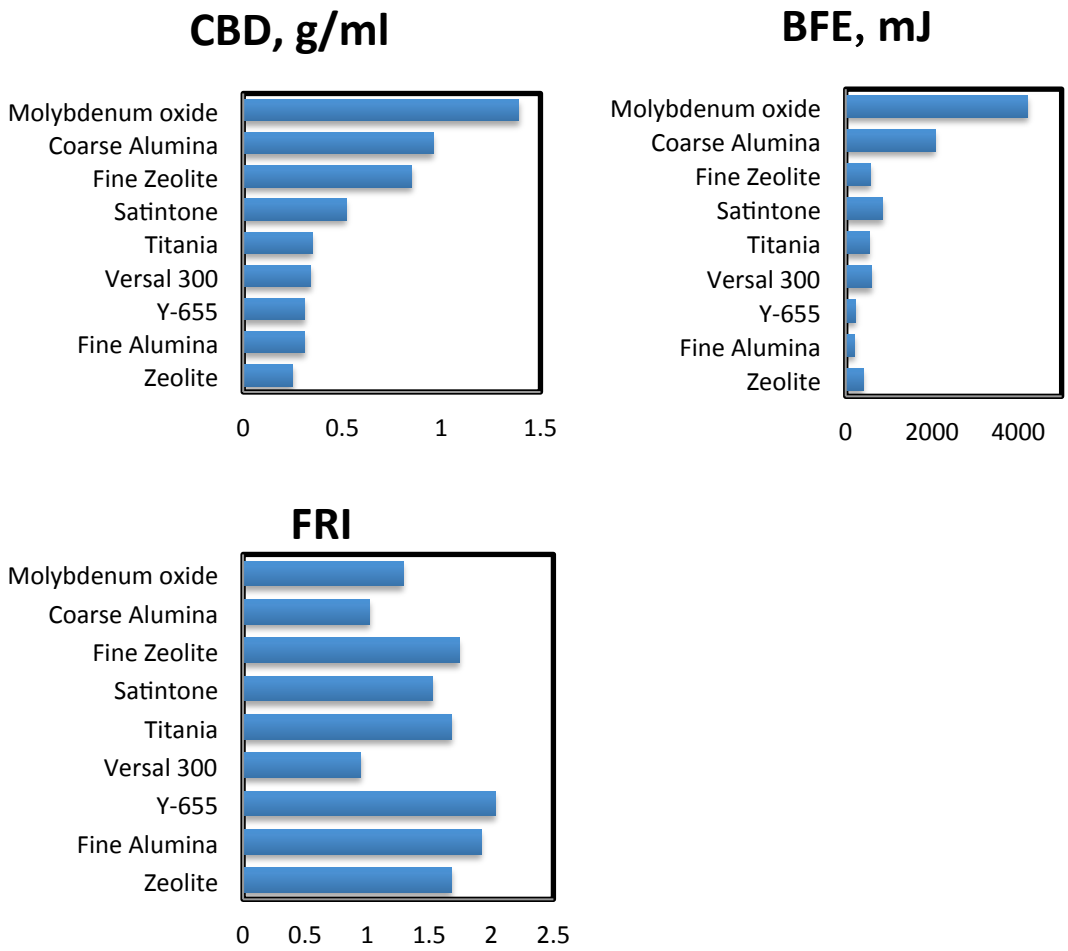

Figure 3-8 Rank of CBD, BFE and FRI

Fig 3-8 suggests that Molybdenum oxide, Coarse Alumina and Fine Zeolite have large CBD, BFE and small FRI. Y-655, Fine Alumina and Zeolite have small CBD, BFE and large FRI.

3.1.4 Cohesion, UYS, MPS and FF

The cohesion, UYS and MPS of 3, 6, 9, 15 kPa are closely clustered on the right side of the correlation loadings ellipse, which means that they have relatively positive correlations. Large cohesion comes with large UYS and MPS. Cohesion as the selected flow property, can represent UYS and MPS. FF with different initial consolidation stress in the ellipse, are on the reverse side. It decreases with increasing cohesion. Flow Function, FF, is a parameter used to rank the flowability of materials.

A small value typically indicates poor flow. While a large value typically indicates good flow. Generally, cohesive materials have poor flowability and non-cohesive materials have good flowability. Take 6 kPa as an example.

Table 3-3 shear cell test at 6 kPa

	coarse alumina	fine alumina	Fine Zeolite	Molybdenum oxide	Satintone	titania	Versal 300	Y-655	Zeolite
Cohesion, kPa-6kPa	0.07	0.78	0.50	1.48	1.23	0.30	-0.09	1.18	1.78
UYS, kPa-6kPa	0.26	2.62	1.59	6.30	4.96	1.52	0	4.17	6.32
MPS, kPa-6kPa	9.23	10.52	8.63	13.57	13.44	13.63	8.33	11.19	12.50
FF-6kPa	35.85	4.01	5.42	2.16	2.73	9.58	0	2.68	1.99

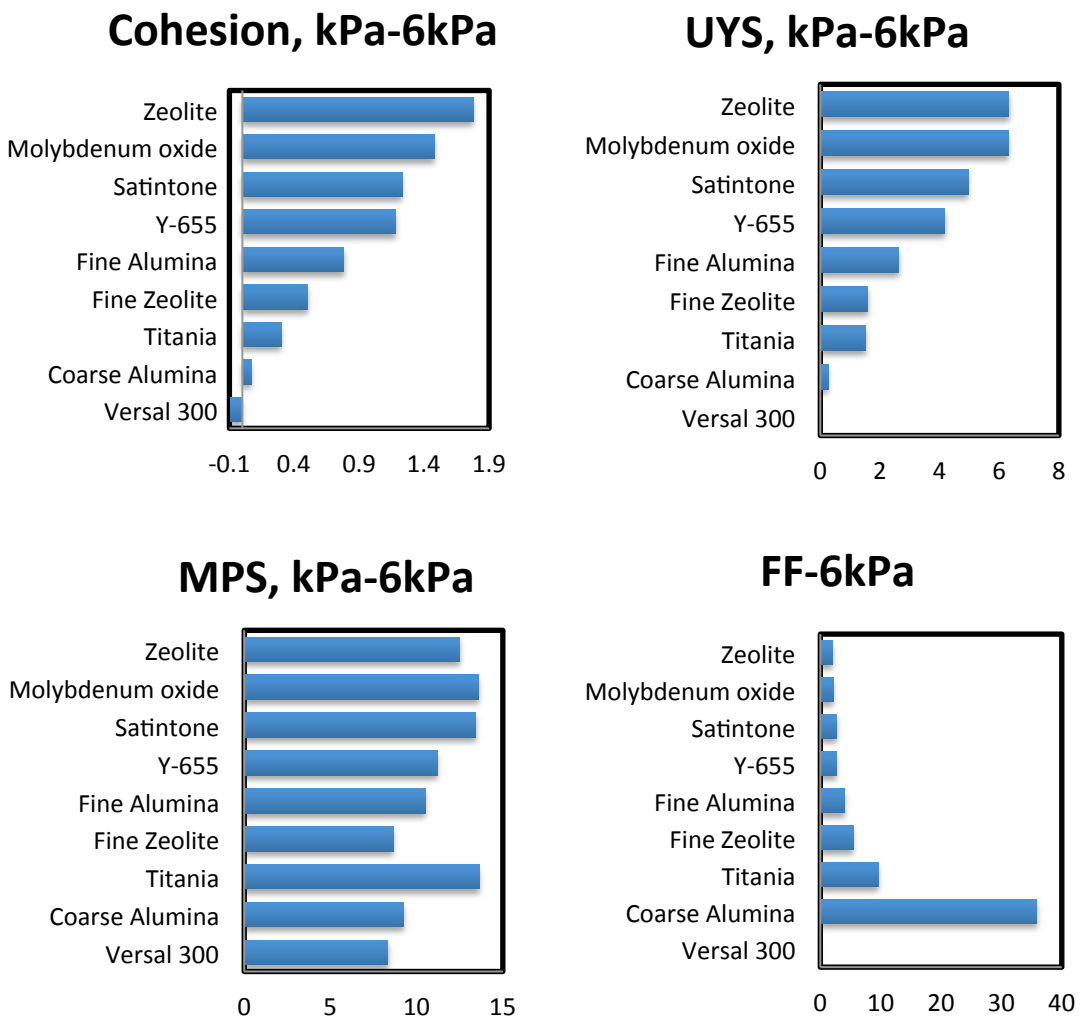

Figure 3-9 Rank of Cohesion, UYS, MPS and FF at 6 kPa

Fig 3-9 suggests that Zeolite, Molybdenum oxide and Satintone are cohesive materials with poor flow function. Titania, Coarse Alumina and Versal 300 are non-cohesive materials with free flow properties.

Table 3-4 cohesion of 9 materials

	coarse alumina	fine alumina	Fine Zeolite	Molybdenum oxide	Satintone	titania	Versal 300	Y-655	Zeolite
Cohesion, kPa-3kPa	0.12	0.42	0.51	1.02	0.93	0.54	-0.04	0.82	0.81
Cohesion, kPa-6kPa	0.07	0.78	0.50	1.48	1.23	0.30	-0.09	1.18	1.78
Cohesion, kPa-9kPa	0.16	0.98	0.56	2.23	1.31	0.66	-0.18	1.51	1.84
Cohesion, kPa-15kPa	0.37	1.39	0.49	2.45	1.01	-0.004	0.28	1.84	1.72

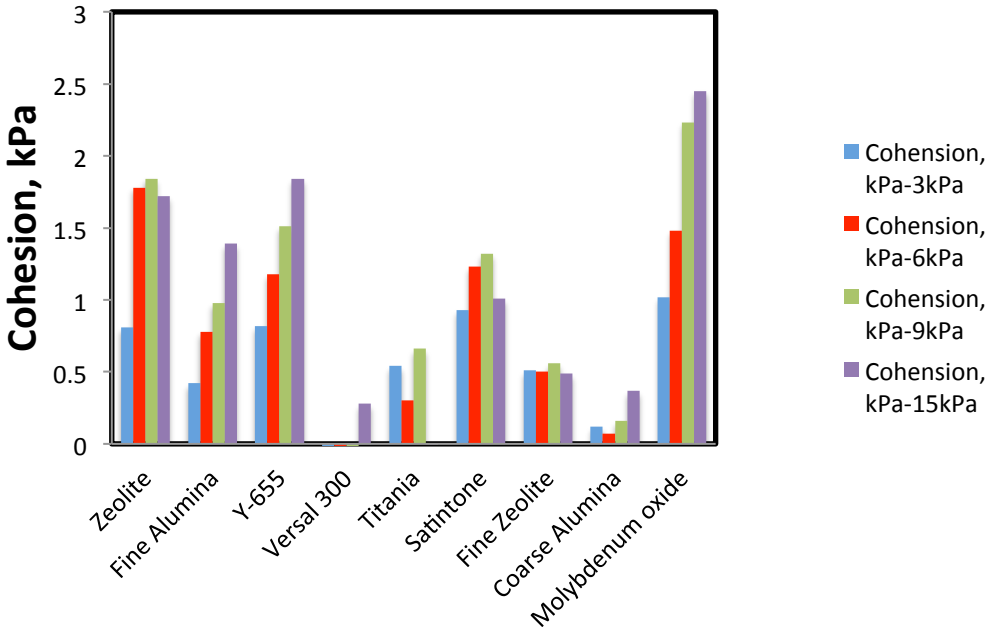

Figure 3-10 histogram of powders' cohesion

Fig 3-10 shows the cohesion of these materials at different initial consolidation stress. We can see from this figure that Molybdenum oxide, Y-655 and Zeolite have higher values of cohesion. Coarse alumina, Fine Zeolite and Titania have the lower

values of cohesion. Since the cohesion at 15 kPa of Versal 300 is positive and low, we can include Versal 300 in the non-cohesive group. Cohesion of Coarse Alumina, Fine Alumina, Molybdenum oxide and Y-655 increase with increasing initial consolidation stress. Some others are flat or have a peak like Fine Zeolite, Satintone and Zeolite. The initial consolidation stress has significant effects on powders' cohesion.

3.1.5 FF and PSD

The FF at 3, 6, 9 kPa and d10, d50, d90 are positively correlated. It seems like powder with large particle size have good flow properties. But we can see from table 3-5 that except Veral 300 and Coarse Alumina, other materials' particle size have little difference. And FF is only one way to show the flowability of powders. Since that, although FF and PSD have positive correlation, it still needs more study to prove that large particle size powder has better flowability.

Table 3-5 particle size distribution data

material	coarse alumina	fine alumina	Fine Zeolite	Molybdenum oxide	Satintone	titania	Versal 300	Y-655	Zeolite
d10	11.16	0.99	0.94	0.76	0.92	0.69	12.35	0.80	0.77
d50	59.37	4.07	3.86	3.71	6.10	2.99	147.83	2.33	2.99
d90	122.19	11.46	5.82	10.31	21.14	10.13	560.05	7.59	10.43

Table 3-6 FF at different pressures

material	coarse alumina	fine alumina	Fine Zeolite	Molybdenum oxide	Satintone	titania	Versal 300	Y-655	Zeolite
FF-3kPa	11.29	3.72	2.77	1.69	1.92	2.85	0	2.07	2.09
FF-6kPa	35.85	4.01	5.42	2.16	2.73	9.58	0	2.68	1.99
FF-9kPa	24.86	4.73	7.47	2.28	3.74	6.52	0	3.14	2.84
FF-15kPa	3.06	4.06	4.50	5.53	7.25	14.16	19.11	26.49	61.19

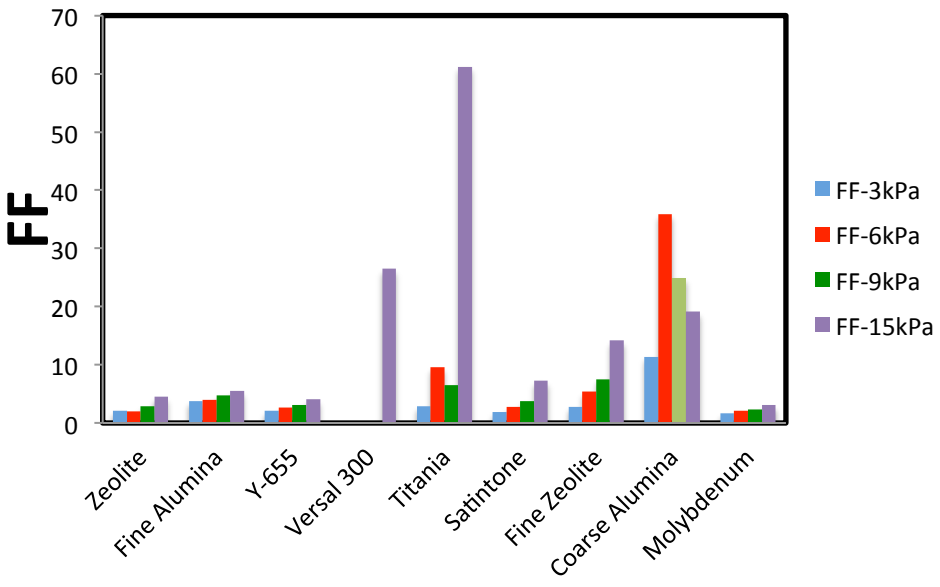

Figure 3-11 histogram of powders' FF at different pressures

Fig 3-11 suggests that some FFs at 15 kPa change too much like Coarse Alumina, Y-655 and Zeolite. Initial consolidation stress has effects on FF and there may be a critical point because FF at 15 kPa are different to other FF.

3.1.6 Materials for feeder tests

Fine Alumina, Coarse Alumina and Satintone were selected for feeder tests. Fine Alumina has small CBD and BFE but large cohesion. Compared with that, Satintone has the similar cohesion but larger CBD and BFE. It means that Fine Alumina is cohesive material that has small density and Satintone is cohesive material with large density. While Coarse Alumina has large CBD and BFE but small cohesion, which means that Coarse Alumina is non-cohesive material with large density, good flowability. Although Versal 300 has some problems with shear cell tests. It can be seen from other data like CPS, PD and SE that Versal 300 is the closest material of these eight to Coarse Alumina. Its behavior can be predicted based on Coarse Alumina.

3.2 Loss-in-weight feeder

3.2.1 Fine Alumina

The capacity of Fine Alumina is around 33 kg/h. Setpoints of 5, 10, 15, 20 and 25 kg/h were selected.

Table 3-6 RSD of Fine Alumina

	Feedrate kg/h	5	10	15	20	25
Helix without screen	RSD 0.1	0.186107	0.107699	0.111439	0.075545	0.052627
	RSD 1	0.13412875	0.04976876	0.05786758	0.02954677	0.01801369
Helix with screen	RSD 0.1	0.085615	0.044499	0.030106	0.022221	0.019271
	RSD 1	0.0431094	0.0204492	0.01546381	0.01105115	0.00967475
Screw without screen	RSD 0.1	0.2185	0.138682	0.080038		
	RSD 1	0.15484996	0.07901415	0.02662074		

PS: RSD 0.1 means the RSD is measured with time interval 0.1s. RSD 1 means the RSD is measured with time interval 1s.

Missing data of Screw with screen was caused by cohesive materials, which blocked inside the tube and stopped the feeder. Same thing happened when feedrate increased to 20 kg/h with Screw without screen.

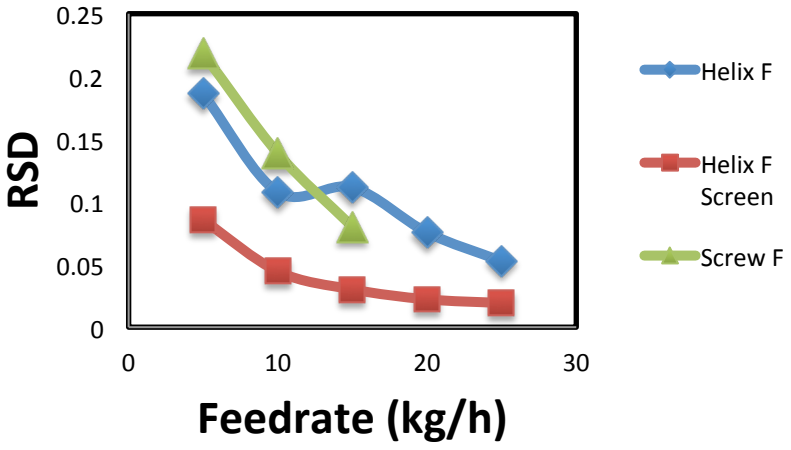

Figure 3-12 RSD 0.1s of Fine Alumina

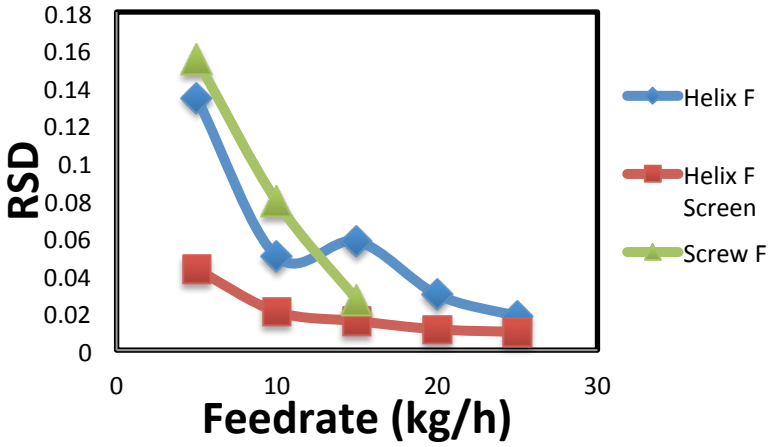

Figure 3-13 RSD 1s of Fine Alumina

From Fig 3-12 we can see RSD always decreases with increasing feedrate. Fluctuations happen at the smallest scale when a small chunk of material (amounts between two consecutive crests, which is called the pitch of a screw) exit the feeder. When speed increases, material passing from more pitches in each time interval, decreasing the size of the fluctuation in the measurement. But we can see from the picture that the red line is almost flat when the feedrate is larger than 10 kg/h. It is to say, increasing feedrate will be helpful for the stability of the powders' flow in the feeder. When it reaches a point, it is meaningless to continue increasing. The feedrate should base on the manufacture requirement.

It can be seen that the Helix with screen has the smallest RSDs. In other words, for materials like Fine Alumina, cohesive and small density, Helix and screen is helpful for the stability of the flow in the feeder. Based on the behavior of Fine Alumina with Screw, we can find the reason from difference in structure between Helix and Screw. The Helix has no center axis, it's empty in the center that makes more room for Fine Alumina to go, less surface contact with Fine Alumina. As for Screw, it has center axis and more surface area than Helix. Fine Alumina is cohesive that it will adhere to the surface of Screw that reduces the effective flow space. Other powders may aggregate in the small room and stop the feeder. The screen will improve this process to act as a barrier that makes the screw with screen refuse working. With Helix, Fine Alumina might be not heavy enough for the Helix to

control its flow performance. The Screen will act as a holder that hinder the powder from flowing out as shown in Fig 3-14. This will improve the control ability of Helix and finally increase the flow stability. Helix with screen is better for cohesive materials like Fine Alumina with small CBD.

Figure 3-14 Fine Alumina feed with screen

3.2.2 Coarse Alumina

The capacity of Coarse Alumina is around 90 kg/h. A big problem happened with Coarse Alumina.

Table 3-7 RSD of Coarse Alumina

	Feedrate kg/h	5	10	15	20
Helix without screen	RSD 0.1	0.225774	0.122365	0.107123	
	RSD 1	0.16707126	0.0874698	0.07993392	
Screw with screen	RSD 0.1	0.224549			
	RSD 1	0.17597774			
Screw without screen	RSD 0.1	0.217281	0.087806	0.050652	0.051616
	RSD 1	0.16181508	0.04879712	0.0179269	0.02901842

Compared with the large feedrate range, the feedrates shown in table 3-7 are too small. That is because that with larger feedrate, there will be noise coming out of the feeder and after a short period of time, the feeder's temperature will increase and then the screw or helix will stop rotating. When disassemble the feeder, there is abrasion inside the tube. It is obvious that the helix or screw was curved by the powder and

friction happened with the inner wall of the tube. Then the energy required for rotating the helix or screw increased with exothermic phenomenon to increase the temperature and finally broke the limit to stop the feeder. It happened with large feedrate because more materials were crossing the tube at the same time that increased the load of the feeder. The Screw is better than Helix because of the center axis. Screw with center axis is stronger than Helix and harder to be curved to some degree. And like mentioned before, the screen acted as a barrier that even increased the load of the feeder. Since the CBD of Coarse Alumina is larger than others. I think it's because of the large CBD that curve the screw and helix. And from Fig 3-15 and Fig 3-16 we can see that the flow behavior of coarse alumina with screw is better than with helix. Since screw is stronger than helix, for materials like Coarse Alumina with large CBD, screw without screen is the optimal combination and low feedrate is better.

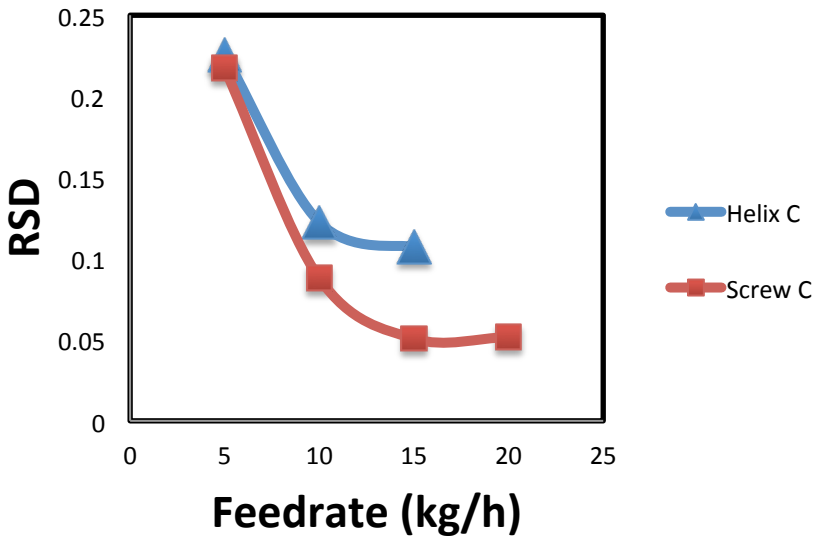

Figure 3-15 RSD 0.1s of Coarse Alumina

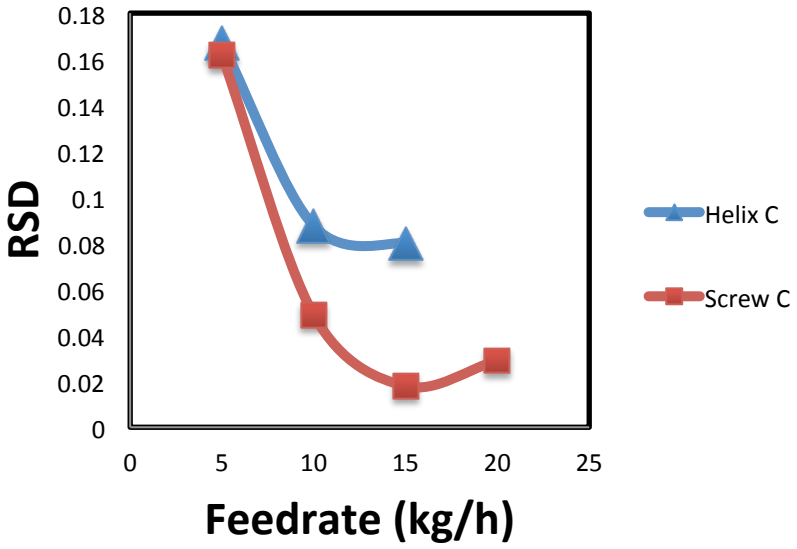

Figure 3-16 RSD 1s of Coarse Alumina

3.2.3 Satintone

The capacity of Satintone is about 20 kg/h.

Table 3-8 RSD of Satintone

	Feedrate kg/h	5	10	15
Helix without screen	RSD 0.1	0.20737	0.098349	0.068299
	RSD 1	0.07238741	0.03783881	0.02982553
Helix with screen	RSD 0.1	0.463938	0.098261	0.068738
	RSD 1	0.17213414	0.02883316	0.02586985
Screw without screen	RSD 0.1	7.207419	1.04516	0.081357
	RSD 1	4.27952549	0.27019062	0.03590044
Screw with screen	RSD 0.1	2.6206	1.281837	0.894393
	RSD 1	0.26854703	0.11360205	0.09791272

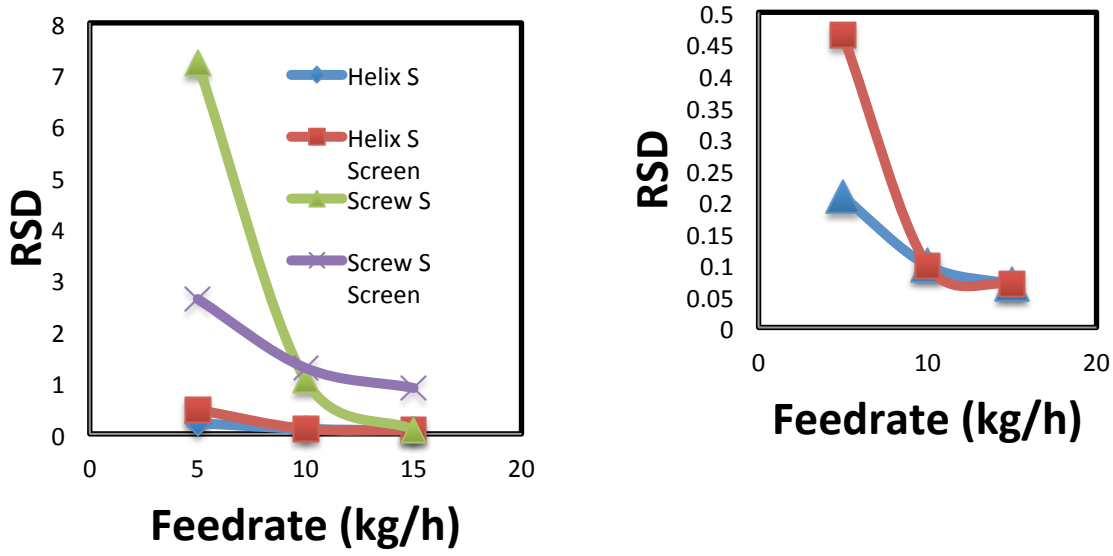

Figure3-17 RSD 0.1s of Satintone

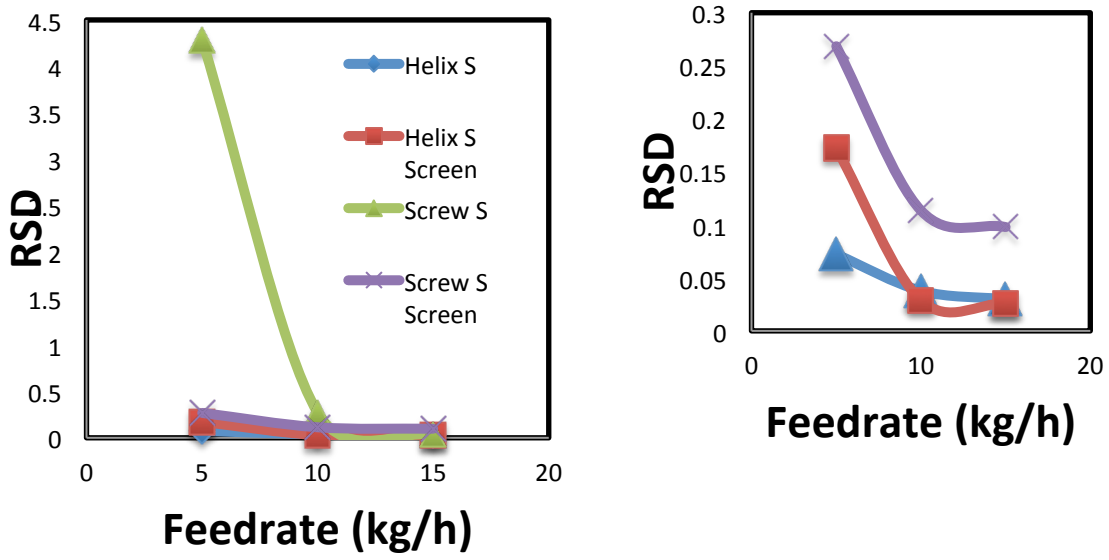

Figure 3-18 RSD 1s of Satintone

The results of helix are better than screw. It is no difference with the results of Fine Alumina that helix is better than screw for cohesive materials because effective flow space is larger and surface contact is smaller. At feedrate 5 kg/h, the helix without screen is better. While when feedrate increased to 10kg/h and 15 kg/h, the RSDs with screen and the RSDs without screen is similar. Screen shows little effects on the flow behavior of Satintone in feeders.

When feeding Satintone, a hole created once in the hopper that no materials went down to the feeder. The feeder stopped because the actually feedrate was less than the minimum setting feedrate. For cohesive materials, this phenomenon called “rat holes” may happen sometimes at higher feedrate because the powders bridge over the screws and act as a barrier to stop powder filling. In this case, no material will enter the screw, and flow will stop.

Figure 3-19 a hole create when feeding satintone

4 Conclusion and future perspective

Nine catalyst support materials were characterized by different flow properties, including particle size distribution, wet and dry impedance, FT4 test such as shear cell, compressibility, permeability and Rep+VFR. Principal component analysis (PCA) was performed to analyze the flow properties and found that CBD has a positive correlation with BFE and a negative correlation with FRI. Possible explanation is that material with large conditioned bulk density requires more energy to flow and has less sensitivity to flow rate change. It is also found that cohesion has positive correlation with UYS and MPS and negative correlation with FF, which shows that cohesive material usually has poor flowability. In addition, initial consolidation stress has large effects on materials' cohesive and flow function. Three materials were selected for feeder tests. Fine Alumina acts as a cohesive material with small bulk density, Satintone is a cohesive material with large bulk density, Coarse Alumina acts as a non-cohesive material with large bulk density. Screw like Helix with less surface area will be helpful for cohesive materials because it can provide more effective flow space and less powder will adhere to the surface. As for feeder control, screen will be better for cohesive materials with small bulk density to hold the material and help better control it. Screw with center axis is better for materials with too much large bulk density because it's stronger and hard to be curved.

For future research, more kinds of materials should be involved, materials with properties: small CBD, medium CBD and large CBD; non-cohesive and cohesive. More feeder tools should be involved, different effective flow space of screw and different void area of screen. Each test can be performed 3 times to calculate the average. Different capacities loss-in-weight feeders should be involved. Three principal component analysis or other statistical methods such as analysis of variance (ANOVA) may be applied to characterize material flow properties.

5 Reference

[1] William E. Engisch, Fernando J. Muzzio, “method for characterization of loss-in-weight feeder equipment,” Powder Technology 228 (2012) 395-403
[2] L.C.R Schneider, I.C. Sinka, A.C.F Cocks, “Characterisation of the flow behavior of pharmaceutical powders using a model die-shoe filling system,” Powder Technology 173 (2007) 59-71
[3] E.C. Abdullah, A.M. Salam and A.R. Aziz, “Cohesiveness and Flowability Properties of Silica Gel Powder,” Physics International 1(1): 16-21,2010
[4] Yanbin Jiang, Shuji Matsusaka, Hiroaki Masuda, Yu Qian, “Development of measurement system for powder flowability based on vibrating capillary method,” Powder Technology 188 (2009) 242-247
[5] Erica Emery, Jasmine Oliver, Todd Pugsley, Jitendra Sharma, Joe Zhou,“Flowability of moist pharmaceutical powders,” Powder Technology 189 (2009) 409-415
[6] AbdulMobeen N. Faqih, Albert W. Alexander, Fernando J. Muzzio, M. Silvina Tomassone,“ A method for predicting hopper flow characteristics of pharmaceutical powders,” Chemical Engineering Science 62 (2007) 1536-1542
[7] Jason Dawes, John F. Gamble, Richard Greenwood, Phil Robbins, and Mike Tobyn, “An investigation into the impact of magnesium stearate on powder feeding during roller compaction,” Drug Development and Industrial Pharmacy 2012 38(1): 111-122
[8] Aditya U. Vanarase, Juan G. Osorio, Fernando J.Muzzio, “Effects of powder flow properties and shear environment on the performance of continuous mixing of pharmaceutical powders,” Powder Technology 246 (2013) 63-72
[9] Qi Zhou, Li Qu, Ian Larson, Peter J. Stewart, David A.V. Morton, “Effect of mechanical dry particle coating on the improvement of powder flowability for lactose monohydrate: A model cohesive pharmaceutical powder,” Powder Technology 207 (2010) 414-421
[10] I.C. Sinka, F. Motazedian, A.C.F. Cocks, K.G. Pitt,“ The effect of processing parameters on pharmaceutical tablet properties,” Powder Technology 189 (2009) 276-284
[11] Matthew Krantz, Hui Zhang, Jesse Zhu, “Characterization of powder flow: Static and dynamic testing,” Powder Technology 194 (2009) 239-245
[12] Xiaowei Fu, Deborah Huck, Lisa Makein, Brain Armstrong, Ulf Willen, Tim Freeman, “Effect of particle shape and size on flow properties of lactose powders,” Particuology 10 (2012) 203-208
[13] Rahul Bharadwaj, William R. Ketterhagen, Bruno C. Hancock, “Discrete element simulation study of a freeman powder rheometer,” Chemical Engineering Science 65 (2010) 5747-5756
[14] Reg Freeman, “Measuring the flow properties of consolidated, conditioned and aerated powders-A comparative study using a powder rheometer and a rotational shear cell,” Powder Technology 174 (2007) 25-33
[15] Kalyana C. Pingali, Kostas Saranteas, Reza Foroughi and Fernando J. Muzzio, “Practical methods for improving flow properties of active pharmaceutical ingredients,” Drug development and Industrial Pharmacy,2009;35(12):1460-1469
[16] Mohamad G. Abiad, David C. Gonzalez, BehicMert, Osvaldo H. Campanella, M. Teresa Carvajal, “ A novel method to measure the glass and melting transitions of pharmaceutical

powders," International Journal of Pharmaceutics 396 (2010) 23-29
[17] Kalyana C. Pingali, M. SilvinaTomassone, and Fernando J. Muzzio, "Effects of Shear and Electrical Properties on Flow Characteristics of Pharmaceutical Blends," AIChE Journal, March 2010 Vol. 56, No. 3
[18] Bumiller Mark, Carson John, Prescott James," A preliminary investigation concerning the effect of particle shape on a powder's flow properties," In World congress on particle technology 4 Sydney, Australia.
[19] Mafalda C. Sarragca, And V. Cruz, Helena R. Amaral, Paulo C. Costa, Joao A. Lopes, " Comparison of different chemometric and analytical methods for the prediction of particle size distribution in pharmaceutical powders," Anal BioanalChem (2011) 399:2137-2147
[20] Rocio Sarrate, Josep Ramon Tico, Montserrat Minarro, Carolina Carrillo, Anna Fabregas, Encarna Garcia-Montoya, Pilar Perez-Lozano, Josep Maria Sune-Negre," Modification of the morphology and particle size of pharmaceutical excipients by spray drying technique," Powder Technology 270 (2015) 244-255
[21] Jason Wiens, Todd Pugsley, "Tomographic imaging of a conical fluidized bed of dry pharmaceutical granule," Powder Technology 169 (2006) 49-59
[22] Haisheng Lin, Ognjen Marjanovic, Barry Lennox, Slobodan Sasic, Ian M. Clegg," Multivariate Statistical Analysis of Raman Images of a Pharmaceutical Tablet," Applied Spectroscopy, Volume 66, Issue 3, Pages 68A-96A and 237-346 (March 2012), 272-281 (10)
[23] Katarzyna Adamska, Adam Voelkel, Karoly Heberger," Selection of solubility parameters for characterization of pharmaceutical excipients," Journal of Chromatography A, 1171 (2007) 90-97
[24] Nan Qu, Ming chao Zhu, Yulin Ren, Sen Dou," Adaptive neuron-fuzzy inference system combined with principal components analysis for determination of compound thiamphenicol powder on near-infrared spectroscopy," Journal of the Taiwan Institute of Chemical Engineers 43 (2012) 566-572